Thermal and Mechanical Properties of Anhydride-Cured Epoxy Resins with Different Contents of Biobased Epoxidized Soybean Oil

F. I. Altuna, L. H. Espósito, R. A. Ruseckaite, P. M. Stefani

Instituto de Investigaciones en Ciencia y Tecnología de Materiales (INTEMA), National Research Council (Consejo Nacional de Investigaciones Científicas y Técnicas), Universidad Nacional de Mar del Plata (UNMdP), Juan B. Justo 4302, B7608FDQ Mar del Plata, Argentina

Received 9 October 2009; accepted 25 July 2010
DOI 10.1002/app.33097
Published online 3 November 2010 in Wiley Online Library (wileyonlinelibrary.com).

ABSTRACT: Thermosetting resins were synthesized by the partial replacement of the synthetic epoxy prepolymer based on diglycidyl ether of bisphenol A (DGEBA) with increasing amounts of epoxidized soybean oil (ESO) with methyltetrahydrophthalic anhydride as a crosslinking agent and 1-methyl imidazole as an initiator. Calorimetric studies showed a drop in the reaction heat with ESO content; this was associated with the lower reactivity of oxirane rings in ESO due to steric constrains. The effects of the replacement of increasing amounts of synthetic DGEBA with ESO on the network properties, such as the storage modulus (E') in the glassy and rubbery regions, glass-transition temperature (T_g), and impact and compressive properties were examined. All formulations were transparent, although phase-separated morphologies were evidenced by scanning electron microscopy observations. The intensity of the transmitted light passed to a minimum at a short reaction time associated with the cloud point and then increased continuously until the refractive index of the dispersed phase approximated that of the continuous phase at complete conversion. The combination of DGEBA with 40 wt % ESO resulted in a resin with an optimum set of properties; E' in the glassy state was 93% of that of the neat DGEBA resin, T_g decreased only about 11°C, and the impact strength increased about 38% without a loss of transparency. © 2010 Wiley Periodicals, Inc. J Appl Polym Sci 120: 789–798, 2011

Key words: biopolymers; mechanical properties; thermal properties

INTRODUCTION

The growing demand for petroleum-based products and the resulting negative impact on the environment plus the depletion of nonrenewable resources have stimulated the use of renewable feedstock in academic research and the chemical industry.[1] Vegetable oils and their derivatives have been identified as potential renewable substitutes for crude oil resources in the production of polymers for many applications.[1,2] Some of these polymers offer performances comparable to petroleum-based ones, and some of them are cheaper and biodegradable.

Among some of the most industrially important vegetable oils, soybean oil emerges as an attractive candidate for such applications. Soybeans are grown predominantly in North and South America, where 33 and 49%, respectively, of the 2007–2008 world supply of beans was harvested.[3] Argentina is the third largest producer of soybeans (54 million tons in 2009–2010), behind the United States and Brazil, and most of the current production is intended for oil production for export (ca. 7.5 million tons in 2009–2010). At this point, the recycling rate of soybean oil into added value products, such as chemicals, biodiesel, and polymer precursors, is constantly increasing.[3,4] Consequently, it would be beneficial from an environmental and economic point of view to combine suitable functionalized soybean oil with petroleum-based materials to develop biobased polymers.[5]

Oils are, as such, not very reactive, and they need further modification to be suitable for most technical applications. Through the chemical modification of soybean oil, a large number of versatile and reactive raw materials can be produced for further polymerization.[1,2] Epoxidation of the double bonds of the fatty acid to obtain epoxidized soybean oil (ESO) is the most important functionalization and can be done by chemical[6] or enzymatic[7] oxidation. ESO is extremely promising as inexpensive renewable

Correspondence to: R. A. Ruseckaite (roxana@fi.mdp.edu.ar).

Contract grant sponsor: National Research Council, Argentina (Consejo Nacional de Investigaciones Científicas y Técnicas); contract grant number: PIP 112-200801-01837.

Contract grant sponsor: Agencia Nacional de Promoción Científica y Tecnológica (ANPCYT); contract grant number: PICT-2006-01560.

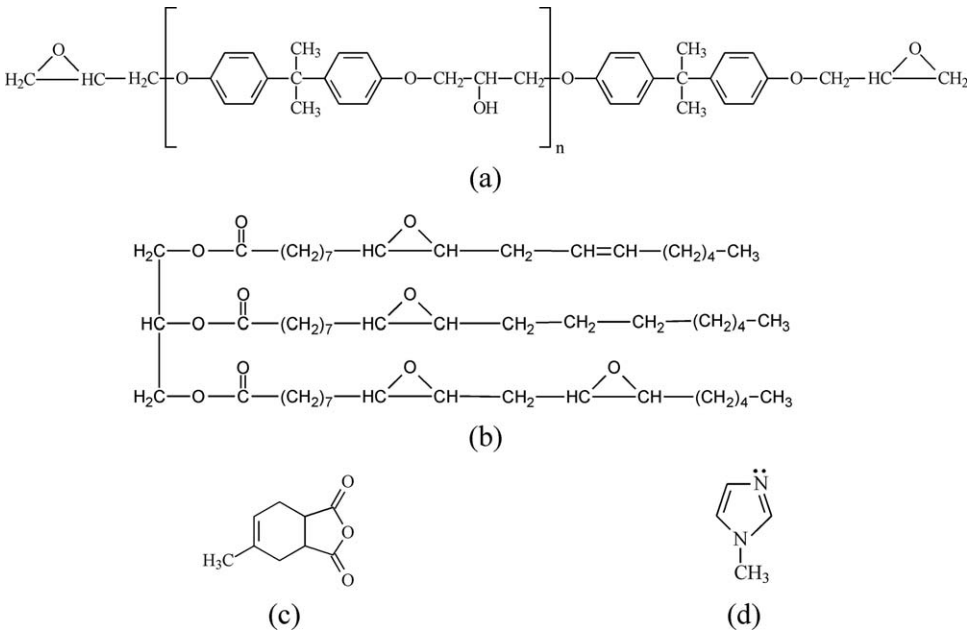

Figure 1 Chemical structure of the materials used in this study.

material for industrial applications because it shares many of the characteristics and properties of conventional epoxy formulations.[8] The feasibility of curing epoxidized vegetable oils (EVOs), either as monomers or as comonomers of petroleum-based epoxy prepolymers, with conventional curing agents, including amines (aliphatic or aromatic),[8–12] thermally latent initiators,[13,14] carboxylic acid anhydrides,[5,15–21] and carboxylic acids,[22,23] is well documented. Information on the curing reaction of EVOs with anhydrides is rather scarce,[15–21] maybe because it is less reactive than amines and, thus, requires higher curing temperatures,[23] although the use of carboxylic anhydride hardeners offer some advantages over amines, including a reduced toxicity and the potential of the produced resins of being hydrolytically degraded[22] or mineralized rather quickly (<100 days) in soil.[24]

In this study, we focused on the structure–properties relationship of resins obtained by the replacement of increasing amounts of synthetic epoxy prepolymer based on diglycidyl ether of bisphenol A (DGEBA) with ESO processed with a stoichiometric amount of methyltetrahydrophthalic anhydride (MTHPA) as a crosslinking agent and 1-methyl imidazole (1-MI) as a catalyst. The effects of ESO on the impact, compression, and thermomechanical properties of the produced epoxy resins are discussed and related with the developed morphologies observed by scanning electron microscopy (SEM) and optical properties, as evaluated by optical light transmission. The main goal of this study was to show that some of the DGEBA–ESO formulations could give rise to transparent, multiphase epoxy networks with improved impact properties.

EXPERIMENTAL

Materials

The epoxy prepolymer was a commercial grade of DGEBA [epoxide equivalent weight (EEW) = 185 g/mol, Araldite GY250, Distraltec, Buenos Aires, Argentina). The hardener MTHPA (>99%, equivalent weight = 166) was obtained from Distraltec. ESO was provided by Unipox S. A. (Buenos Aires, Argentina, iodine value = 2.4, EEW = 242, 929 g/mol). Both chemicals, DGEBA and ESO, were dried *in vacuo* overnight before use. 1-MI (>99%) was purchased from Huntsman (Buenos Aires, Argentina) and was used as received. The chemical structures of DGEBA, ESO, MTHPA, and 1-MI are shown in Figure 1.

Synthesis of the DGEBA–ESO networks

ESO was used to replace 20, 40, 60, 80, and 100 wt % of the DGEBA in the resin formulations. Blending was performed in a one-stage process by the direct mixing of epoxy monomers with a stoichiometric amount of MTHPA and catalytic amounts of 1-MI (3 wt % on the basis of the anhydride weight).[15] All formulations were placed in a glass round-bottom flask and heated at 50°C for 30 min. The mixing process was carried out under reduced pressure (~ 10

mmHg) to reduce the volume of air bubbles entrapped in the bulk. Subsequently, the reactive mixture was transferred into steel molds coated with antiadherent paper, which were then placed in a convection oven Yamato DKN400 (San Francisco, California) and subjected to a two-step curing process selected according to preliminary calorimetric studies: 130°C for 1 h and then 190°C for 3 h. The specimens were cut to suitable dimensions for mechanical tests.

Characterization

Calorimetric studies were performed in the nonisothermal mode with differential scanning calorimetry (DSC; Shimadzu DSC 50, Kyoto, Japan). Dynamic experiments were carried out from room temperature to 250°C at a heating rate of 10°C/min and under a nitrogen atmosphere (20 cm^3/min). Fourier transformed infrared (FTIR) spectroscopy spectra were recorded on a Mattson Instruments Genesis II FTIR spectrometer (Madison, WI). All runs were performed between 400 and 4000 cm^{-1}. For the reactive samples, analysis was performed on thin films spattered on NaCl crystals. An attenuated total reflection accessory with a diamond attenuated total reflection crystal was used to analyze the cured samples with 32 scans at a resolution of 4 cm^{-1}. The dynamic mechanical properties were measured with dynamic mechanical analysis (DMA; PerkinElmer UNIX DMA 7, Norwalk, Connecticut). Specimens 1.5 mm thick, 3 mm wide, and 20 mm long were tested in a three-point-bending configuration. The storage modulus (E'), loss modulus (E''), and loss factor (tan δ) as a function of the temperature were obtained at a heating rate of 10°C/min from −25 to 190°C and at a fixed frequency of 1 Hz. Charpy-type impact tests were performed in an instrumented falling weight impact tester (Fractovis, Ceast, Turin, Italy). Rectangular, V-notched specimens with nominal dimensions (S × W × B = 120 × 13 × 7.5 mm^3, where S is the length, W, the width and B is thickness) were struck by an impact mass of 24 kg at an impact speed of 0.5 m/s at room temperature. The impact strength was calculated as the ratio between the energy consumed (area of the load vs deformation curve) and the resistant area of the sample (ASTM D 6110-040).[25] The distance between supports was set to 95 mm. The average results obtained from 10 samples per material are reported as the impact strength. Compression tests were preformed in accordance with the procedure in ASTM D 695-02.[26] Cylindrical specimens (15 mm in diameter and 15 mm in height) were cut from the molded samples. Compression tests were conducted at a crosshead speed of 1.3 mm/min and at room temperature with an Instron 4467 universal testing machine (Buckinghamshire, England). The top and bottom surfaces of testing specimens were previously lubricated with molybdenum disulfide to minimize the friction with each plate of the machine. The load versus displacement data were used to determine the compressive yield strength (σ_c) and compressive modulus (E_c). The results are the average of five measurements for each composition. The failure impact surfaces were observed with a JEOL JSM-6460LV (Tokyo, Japan) scanning electron microscope at a 15-kV accelerating voltage. Before observation, the fracture surfaces were sputter-coated with a thin layer of gold to prevent charging under the electron beam. Transmission optical microscopy was used to determine the evolution of the intensity of the transmitted light during the curing of the reactive mixtures with a Leica DMLB (Wetzlar, Germany) microscope equipped with a Linkam THMS 600 (Tadworth, England) hot-stage. The hot-stage was programmed to reproduce the temperature conditions used in the convection oven, and the light transmitted through 0.50 mm thick samples was detected by a photodiode. The experimental data were collected as the intensity of the transmitted light versus time traces.

RESULTS AND DISCUSSION

Study of the curing process

Comprehensive studies of the curing behavior of epoxy–anhydride mixtures are well reported in the literature.[27–30] The main disadvantage of noncatalyzed epoxy–anhydride mixtures is the long reaction time at high temperatures needed to obtain resins with optimal properties.[28] Thus, strong Lewis bases, such as tertiary amines or imidazoles, are usually required to overcome this drawback. However, the mechanism in the presence of Lewis bases is less clear. Rocks et al.[28] postulated a mechanism assuming that the reaction of the tertiary amine with the epoxide ring to form a zwitterion contained an ammonium cation and an alkoxide. Propagation took place via the reaction of the carboxylate ion with an epoxy group, with the formation of a new alkoxide anion. Thomas et al.[30] proposed an anionic mechanism initiated by the ring-opening of epoxy rings by the tertiary amine, with the ester–alkoxide anion as the propagating species. According to Boquillon and Fringant,[15] imidazole was more effective than tertiary amines in initiating the polymerization of epoxidized linseed oil (ELO) because the resulting networks exhibited a higher anhydride conversion. Because the structures of ESO and ELO were quite similar, 1-MI was selected as the initiator of the coreaction of ESO with DGEBA with stoichiometric amounts of MTHPA. The epoxy–anhydride curing process was analyzed by nonisothermal DSC

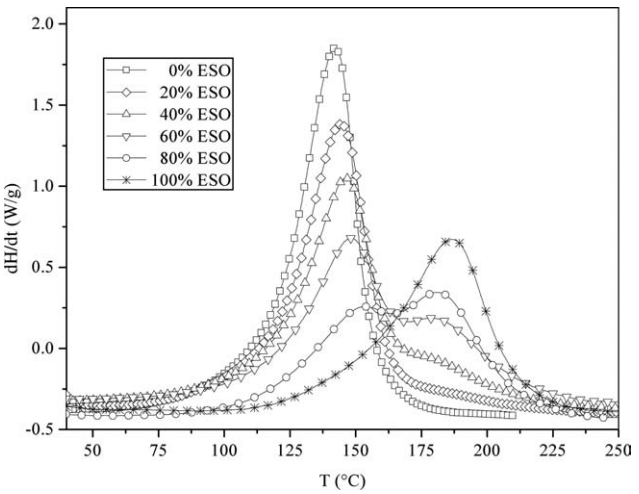

Figure 2 Dynamic thermograms of the DGEBA–ESO–MTHPA systems (10°C/min and N_2 atmosphere; T = temperature; dH/dt = variation of the enthalpy with the time normalized by the initial mass).

experiments, and the obtained thermograms for different weight ESO contents are shown in Figure 2. Table I shows the peak maximum temperature (T_p) and the total reaction heat (ΔH) values. As shown in Figure 2, the neat DGEBA–MTHPA and ESO–MTHPA formulations exhibited single exothermic reaction peaks attributed to the epoxy–anhydride curing reaction at 142 and 187°C, respectively. According to data reported in Table I, the MTHPA-cured ESO resin showed a high peak temperature but a lower reaction heat. This was ascribed to the hindered oxirane functionalities, which were in the middle of the fatty acids in the ESO molecule[13] and reacted sluggishly with nucleophilic curing agents in the stoichiometrically balanced polymerizations. The addition of ESO to the DGEBA–MTHPA mixture changed the shape of the exothermic peaks. Two partially overlapped peaks were clearly distinguished, particularly for ESO contents higher than 40% (Fig. 2). The addition of increasing amounts of ESO shifted the maximum temperature of the first exothermic event to higher values. As stated before, this result was attributed to the polymerization of ESO at higher temperatures compared with that of DGEBA because of the less reactive oxirane rings centrally placed in long aliphatic chains of ESO. This effect was accompanied by a decline in the total heat of reaction (Table I). This behavior was in agreement with results previously reported for other DGEBA–ESO systems crosslinked with isophorone diamine.[11] Total enthalpy values were expressed in kilojoules per equivalent, with the EEW involved in the epoxy–anhydride reaction taken into account (Table I). The ΔH values obtained in this study were higher than those reported for the curing reaction of ELO with 3,4,5,6-tetrahydrophtalic anhydride (THPA) anhydride in the presence of 2-methylimidazole (2-MI) (0.5% w/w)[15] and those obtained by dos Santos Martini et al.[20] for linseed oil epoxidized methyl esters cured with THPA and 2-MI. Differences in the ΔH values were related to differences in the molecular structures of the vegetable oils.

The evolution of the reactive groups that participated in the curing reaction was followed by FTIR spectroscopy (Fig. 3). The most significant bands in the initial DGEBA–MTHPA reactive mixture were the stretching vibrations at 916 and 970 cm^{-1} associated with the terminal epoxy moieties in DGEBA and the two intense axial deformation bands of carbonyl groups at 1780 and 1850 cm^{-1}, which corresponded to MTHPA [Fig. 3(a)].[28] In addition to the distinctive MTHPA carbonyl stretching peaks, the ESO–MTHPA reactive mixture exhibited a strong C=O stretching vibration at 1732 cm^{-1}, which was assigned to triglyceride carbonyl stretching in ESO,[18] and absorption peaks of the internal epoxy groups at 820 and 844 cm^{-1}.[19] The completion of the curing reaction was characterized by the disappearance of the anhydride and epoxy absorption peaks with the concomitant appearance or relative increment (for the case of ESO-containing samples) in the carbonyl ester band intensity [1732 cm^{-1}; Fig. 3(b,c)]. The disappearance of epoxy rings associated with ESO at 820 and 844 cm^{-1} was difficult to verify because this absorption was superimposed with that attributed to the *p*-phenyl group from DGEBA [Fig. 3(c)]. All of these observations provided evidence that the polymerization reaction had occurred. Small characteristic OH bands around 3400 cm^{-1} appeared in the final spectrum of all of the samples. This indicated that some internal alkoxide ions produced during the curing reaction were more hindered to react with the anhydride and, thus, could be converted into OH groups by the action of traces of moisture.

Thermomechanical behavior

Figure 4 shows the temperature dependence of E', E'', and tan δ for the neat DGEBA and ESO resins and DGEBA–ESO cured copolymers. Table II

TABLE I
T_p and ΔH Values of the MTHPA-Cured DEGBA–ESO Mixtures Determined from Dynamic Thermograms at 10°C/min

ESO (%)	ΔH (kJ/equiv)	T_{p1} (°C)	T_{p2} (°C)
0	67.1	142	—
20	63.5	144	—
40	61.9	146	176
60	59.8	148	179
80	58.4	154	181
100	55.2	—	187

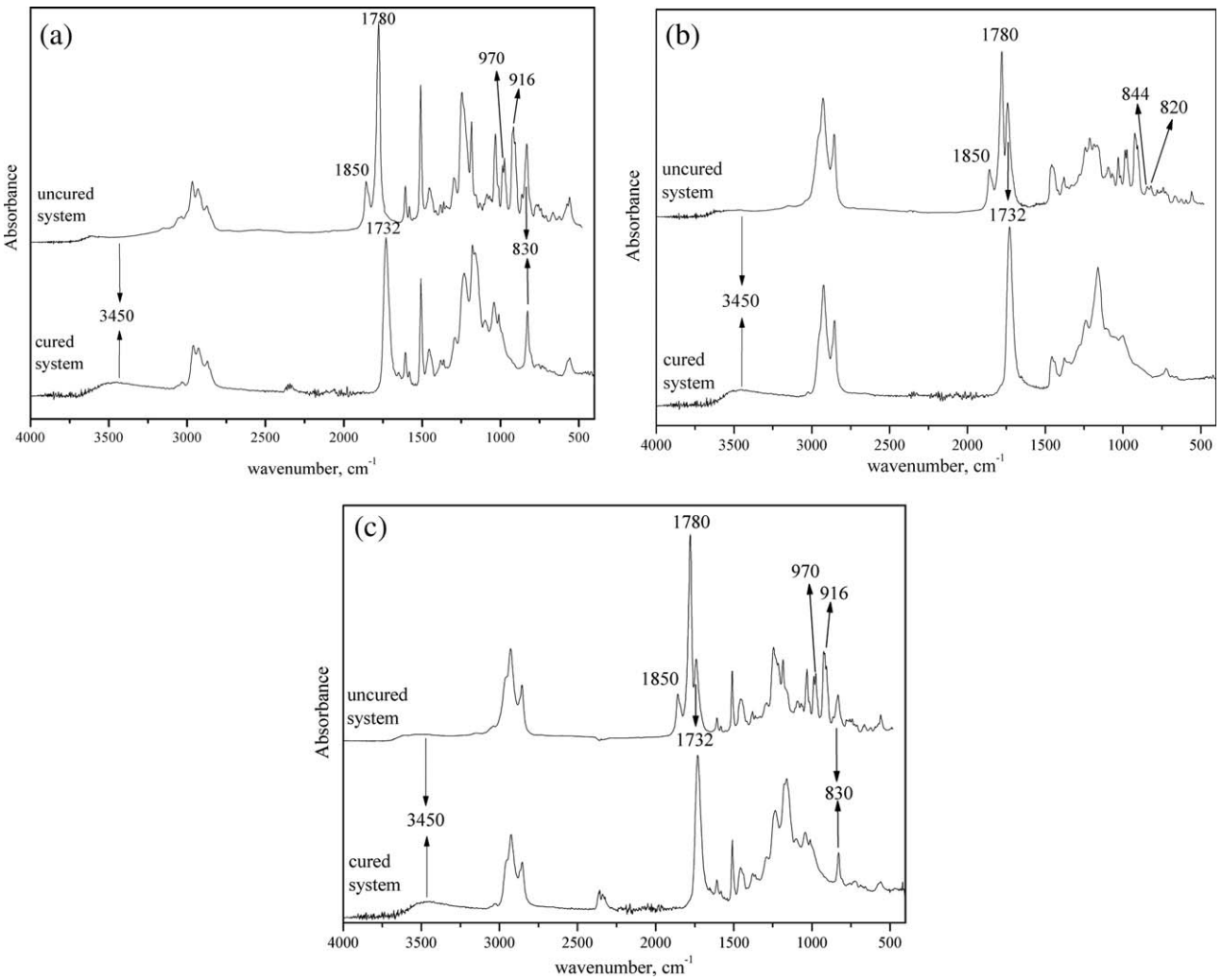

Figure 3 FTIR spectra of the DGEBA–ESO–MTHPA reactive mixtures at time = 0 and at complete conversion (a) 0, (b) 100, and (c) 40% ESO.

summarizes some parameters calculated from these curves. Changes in E' with temperature for different ESO contents are shown in Figure 4(a). At low temperatures, there was a glassy state with E' staying at a high modulus plateau and a rubbery state at temperatures higher than the glass-transition temperature (T_g) with a lower E' [Fig. 4(a), Table II]. In the region of high temperatures, E' was almost constant; this indicated the presence of stable crosslinking points and implied that the epoxy groups scarcely remained unreacted in these materials; this was in agreement with the absence of residual heat in the dynamic DSC runs. As shown in Figure 4(a), the E' values at 30°C decreased with the addition of ESO from 2.43 ± 0.13 to 1.34 ± 0.16 MPa for 0 and 100% ESO, respectively. Therefore, the replacement of increasing amounts of DGEBA with ESO gave rise to an increase in the chain mobility within the DGEBA–ESO–MTHPA networks. The E' values at T_g + 50°C for the neat DGEBA and ESO networks did not exhibit significant differences; this suggested that both neat resins had similar crosslinking densities.

T_g was measured from the maximum of the E'' curve [Fig. 4(b)], which was associated with the α-relaxation of each sample. All formulations exhibited T_g values above room temperature. The neat DGEBA network showed a well-defined α-relaxation at 108°C, which shifted to lower temperatures with increasing ESO content until a value of 57°C was reached for the neat ESO resin (Table II). Changes in T_g could have been caused by the plasticization effect of ESO due to the more flexible and elastic structure the ESO compared to that of DGEBA (Fig. 1). The T_g values obtained for MTHPA-cured DGEBA–ESO networks were in the same range as those previously reported for ESO81–phthalic anhydride–triethylamine resin[16] but lower than those observed for diglycidyl ether of bisphenol F–ELO–MTHPA resin[9] and ELO–

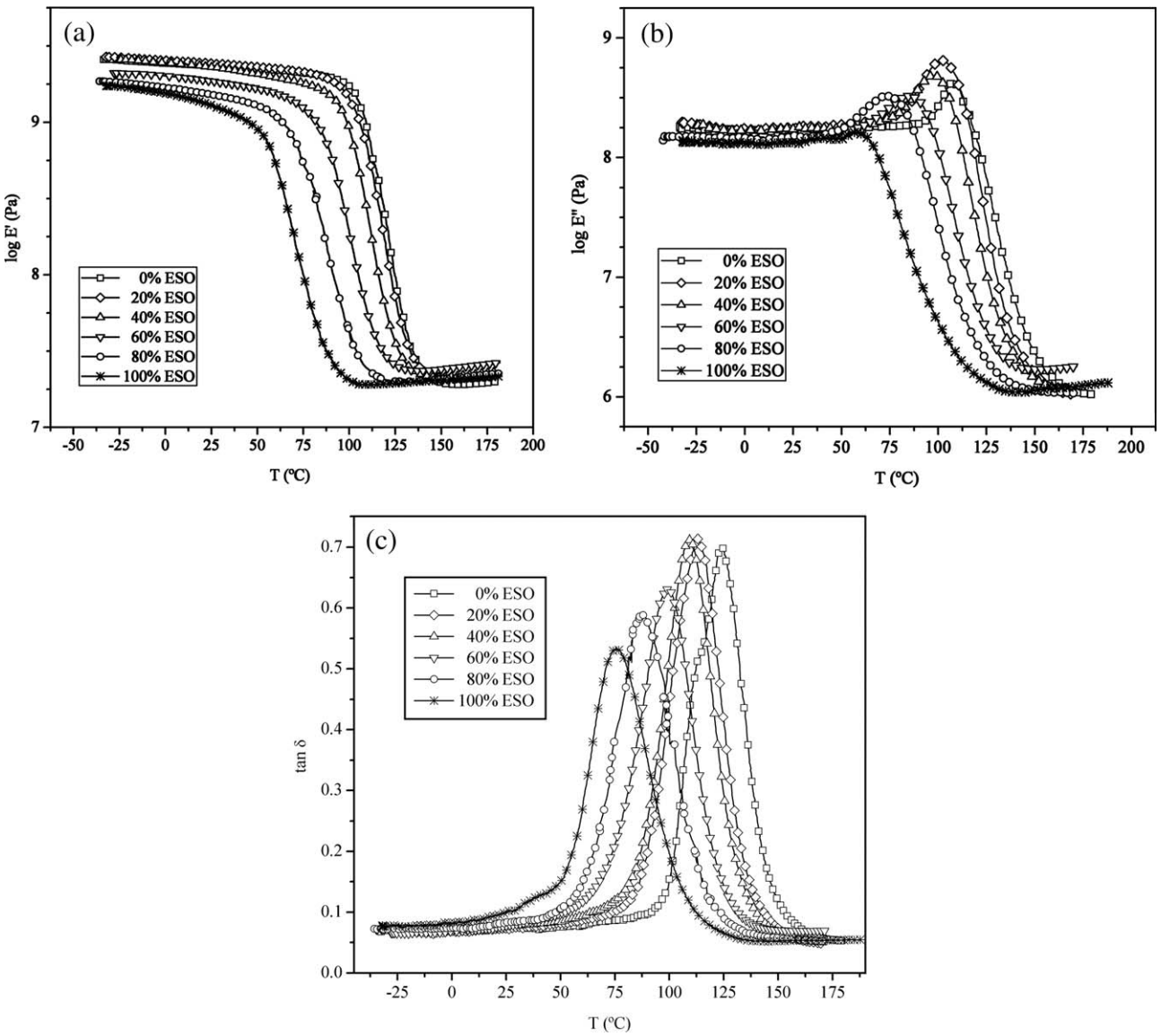

Figure 4 Effect of the replacement of increasing amounts of DGEBA with ESO in the MTHPA-cured epoxy resins on (a) E', (b) E'', and (c) tan δ versus temperature (T).

MTHPA;[15] this may have been due to the lower EEW and higher epoxy functionality of ELO compared to ESO.

Figure 4(c) shows the dependence of tan δ with temperature for different amounts of ESO replacing DGEBA. The symmetry of the tan δ peaks was an indication of the complete curing of the anhydride-cured epoxy matrix. The peak widths increased, whereas their heights decreased with increasing ESO content. This suggested that the biobased resin had a broader glass-transition region because of the heterogeneous DGEBA–ESO–MTHPA network,[9,16,17] although DMA measurements did not give any evidence of phase separation. The heterogeneous nature of the DGEBA–ESO networks is further discussed

TABLE II
Physical and Thermomechanical Properties of the MTHPA-Cured Epoxy Resins with Increasing Amounts of ESO: T_g and E' Values in the Glassy and Rubbery States

ESO (%)	T_g (°C)[a]	E' (T_g + 50°C; MPa)	E' (30°C; GPa)
0	108	19.4 ± 0.4	2.43 ± 0.13
20	102	22.6 ± 1.9	2.41 ± 0.21
40	97	22.2 ± 2.6	2.26 ± 0.11
60	85	24.3 ± 1.9	1.82 ± 0.15
80	72	20.7 ± 2.5	1.48 ± 0.10
100	57	19.1 ± 1.2	1.14 ± 0.16

[a] Determined from the maximum of E'' versus temperature curve.

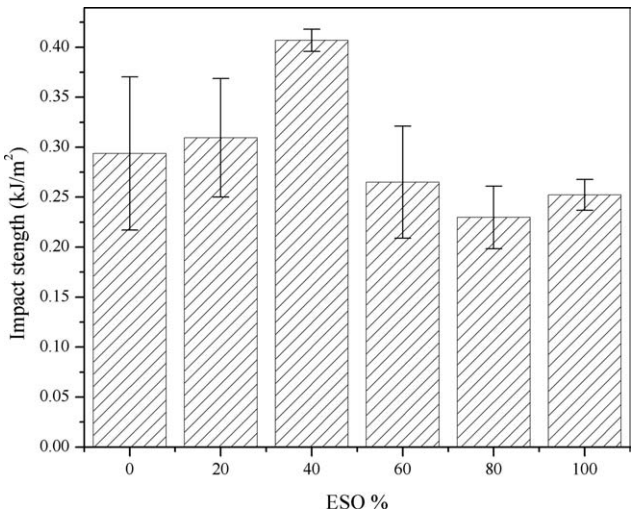

Figure 5 Impact properties of the DGEBA–ESO–MTHPA resins as a function of the ESO content.

with respect to the impact tests and SEM micrographs in the following section.

Impact behavior and microstructure

The results of the impact strength tests of the cured DGEBA–ESO bioresins as a function of ESO content are shown in Figure 5. The impact strength increased, and the value attained a maximum for 40% ESO, which was about 38% higher than that of the neat DGEBA resin (0.29 ± 0.08 J/m^2). Beyond this value, the impact strength declined until it reached that of the ESO–MHTPA resin (0.25 ± 0.0.2 J/m^2). Our results differed from those reported by Miyagawa et al.[9] for diglycidyl ether of bisphenol F–ELO–MTHPA, where the impact strength was almost constant up to 60% and decreased with further addition of ELO. This behavior was attributed to the lack of phase separation in all of the formulations, as we concluded from the SEM results. On the contrary, our findings agreed with those of Ratna,[31] who reported a maximum impact strength at 20 phr ESO for blends with DGEBA crosslinked with tris-2,4,6-(*N*,*N*-dimethyl amino methyl) phenol, associated with a two-phase microstructure.

To give a plausible explanation for the impact results found herein, the failure surface of the DGEBA–ESO networks were observed by SEM, and microphotographs are shown in Figure 6. The failure surface of the DGEBA–MTHPA resin was featureless [Fig. 6(a)]. In contrast, the surface of the bioresin containing 40% ESO exhibited a much rougher surface [Fig. 6(b)]. Also, the same sample observed at higher magnification [Fig. 6(c)] revealed dispersed domains within the matrix. These dispersed particles acted as center of dissipation of mechanical energy by shear yielding and gave a maximum in the impact strength value.[31] The DGEBA and ESO neat resins did not have any phase separation; thus, they displayed a lower impact strength (Fig. 5). The decrease in impact strength above 40% ESO could be ascribed to phase inversion.[31]

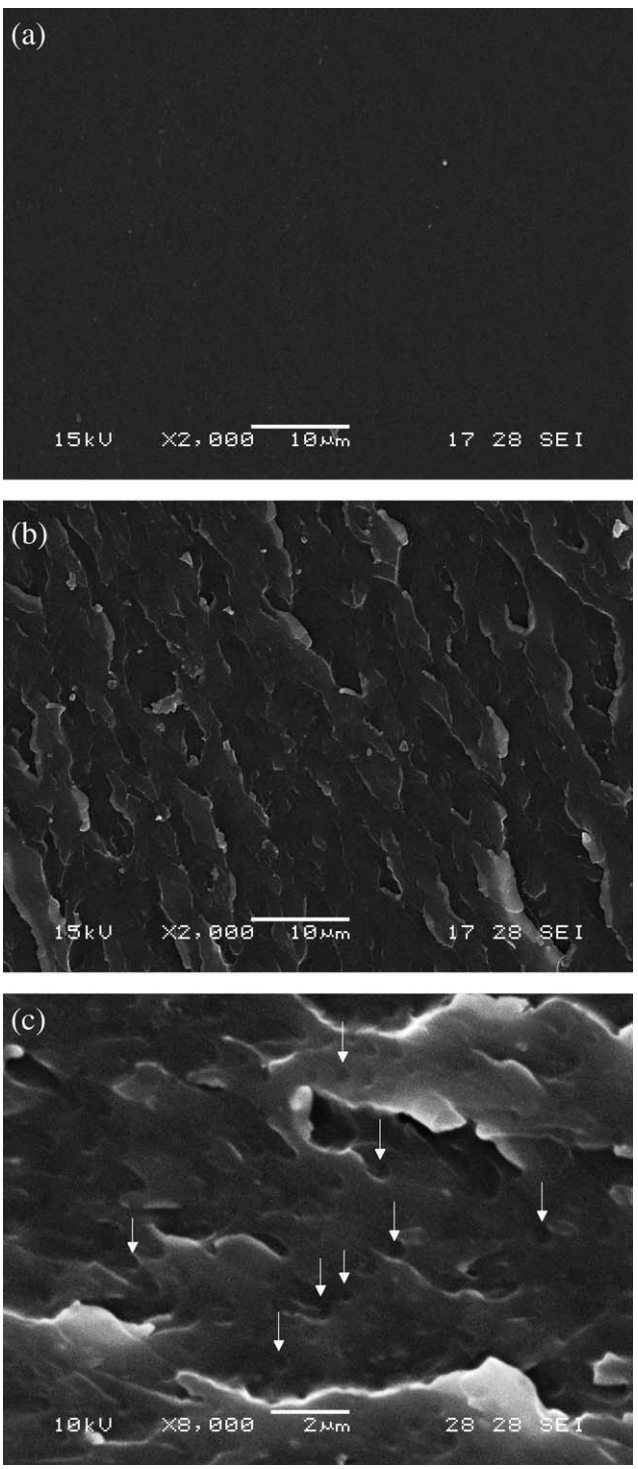

Figure 6 SEM micrographs of the failure impact surface of the (a) DGEBA–MTHPA resin (magnification = 2000×), (b) DGEBA–40% ESO–MTHPA (magnification = 2000×), and (c) DGEBA–40% ESO–MTHPA (magnification = 8000×).

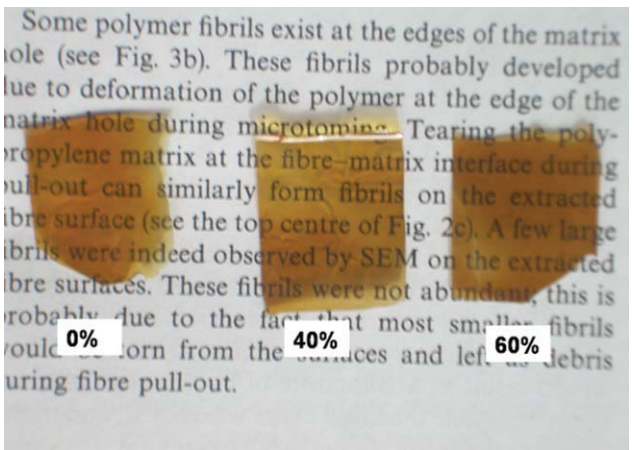

Figure 7 Macroscopic aspect of the DGEBA–ESO–MTHPA resins. [Color figure can be viewed in the online issue, which is available at wileyonlinelibrary.com.]

The obtained results could be explained with the assumption that the reactivity of the internal epoxy rings in ESO was lower compared to that of DGEBA because of steric hindrance; consequently, the initially homogeneous DGEBA–ESO reactive mixtures underwent phase separation induced by the DGEBA–MTHPA reaction, but some amount of ESO reacted with DGEBA remained within the continuous phase, imparting its plasticizing effect. Because MTHPA reacted with the epoxy rings from both DGEBA and ESO, the dispersed particles may have also contained chemically bonded DGEBA segments. Interestingly and contrary to the results reported for other phase-separated epoxy–EVO systems,[5,9,13] all samples remained transparent at complete conversion with a yellow brownish coloration due to 1-MI (Fig. 7). According to Mizutani,[32] two reasons were postulated for this: (1) the diameter of the dispersed phase was lower than the wavelength of the visible light, or (2) in the phase-separated structure, the refractive index of the dispersed phase attained a value close to that of the matrix after complete conversion. The average diameter of the dispersed domains of 40% ESO and 60% ESO (as measured from the SEM micrographs before postcuring) were 0.35 ± 0.07 and 4.45 ± 0.71 μm, respectively; this showed that the size of the dispersed phase was equal to or higher than the wavelength of the visible light (400–800 nm) and implied that transparency could not be ascribed to the size of the dispersed phase. Therefore, we monitored the phase-separation process by following the intensity of the transmitted light versus time curves for the DGEBA–ESO reactive mixtures containing 40 and 60% ESO submitted to the same curing cycle used in the convection oven, and the results are depicted in Figure 8. Initially, the reactive mixtures were transparent because of the miscibility of ESO in DGEBA; this was in agreement with the small differences in the solubility parameters calculated by the group contribution[33] (18.00 $MPa^{1/2}$ for ESO and 21.71 $MPa^{1/2}$ for DGEBA). As the reaction proceeded, samples containing ESO showed a sharp decrease in the intensity of the transmitted light characteristic of the cloud point.[34] The two-phase morphology at the minimum intensity of light transmitted for 40% ESO was confirmed by SEM observation (see the top inset in Fig. 8). However, after this minimum, the intensity of the transmitted light increased continuously until it attained approximately the same value as that of the DGEBA neat resin. The increment in the refractive index of the dispersed phase with

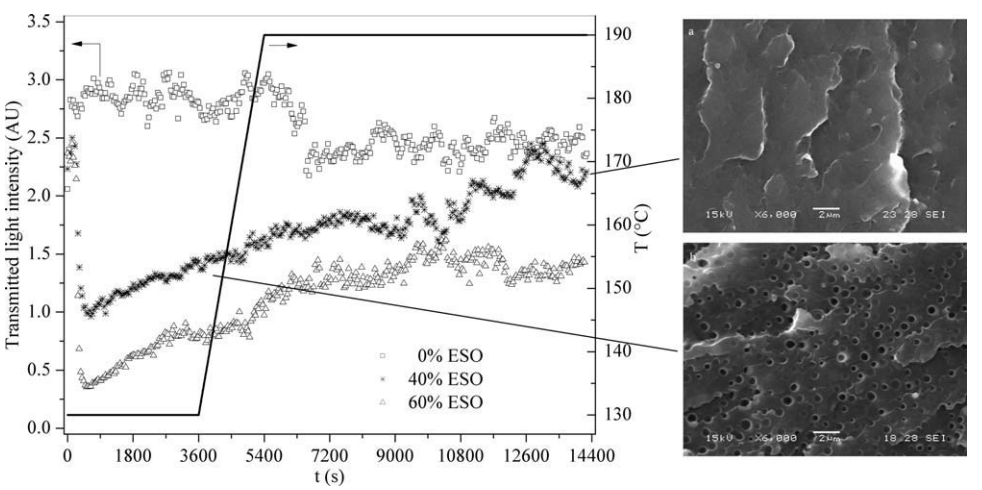

Figure 8 Evolution of the intensity of the transmitted light as a function of the curing cycle for the DGEBA–40% ESO–MTHPA and DEGBA–60% ESO–MTHPA bioresins. (Top inset) SEM micrograph of the morphology generated in DGEBA–40% ESO before postcuring step. (Bottom inset) SEM micrograph of the morphology developed in DGEBA–40% ESO at complete conversion (T = temperature and t = time).

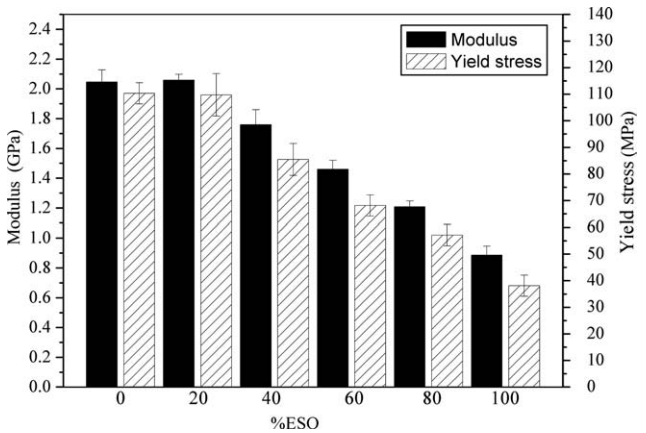

Figure 9 E_c and σ_c as a function of ESO in DGEBA–ESO–MTHPA.

conversion led to transparent materials at complete conversion (see the bottom inset in Fig. 8). Similar behavior was found in other multiphase epoxy systems.[32,34]

Compression properties

Because of the inherent brittleness of the obtained resins at ambient temperature, the yield strength could not be attained in flexural or tensile mode. Therefore, their mechanical parameters were determined in compression mode, and the results are depicted in Figure 9. E_c of the cured samples decreased with the ESO content; this confirmed the previously indicated trend observed for the E' values determined by DMA. Two factors cause a drop in the modulus in systems that can phase-separate:[35] an increase in the volume fraction of the more ductile dispersed phase and a decrease in the rigidity of the continuous phase due to the copolymerization with flexible molecule of ESO. Jim and Park[36] proposed that the reduction in the modulus of the epoxy–ESO network at room temperature was caused by the more flexible structure of the coreacted ESO. This explained the behavior of the bioresins in our study containing 20 and 80% ESO. Contrarily, for 40 and 60% ESO, both factors might have contributed to the modulus reduction. The experimental E_c values of the samples with high ESO contents were in the same range as those reported by other authors for amine-cured[9] and homopolymerized[13,14] epoxy systems. The σ_c values (Fig. 9) remained almost constant up to 20% ESO and dropped for higher amounts of ESO. In addition, the ESO–MTHPA system exhibited a σ_c value 65% lower than that of DGEBA–MTHPA. These results could be explained as follows: the yield of the epoxy networks occurred mainly because of the shear yielding process, which was favored by the addition of more flexible ESO chains and the presence of a dispersed phase.

CONCLUSIONS

Transparent epoxy resins based on DGEBA partially replaced by biobased ESO were prepared with MTHPA–1-MI as a crosslinking–initiator system. E' in the glassy state and T_g decreased with ESO, whereas E' in the rubbery phase was almost constant. No other thermal event besides T_g was detected in the E'' or tan δ traces. However, impact strength exhibited a maximum for 40% ESO, which was ascribed to phase separation, as evidenced by SEM observations. The transparency of the produced resins in the whole composition range was ascribed to the increment of the refractive indices of the dispersed phase with the conversion to attain values close to that of the continuous phase. In terms of the performance, the formulation with 40% ESO exhibited the best set of properties (impact strength was upgraded about 38%, E' was almost invariable, and T_g only decreased 11°C), with the benefit of being transparent and more environmentally sound than petroleum-based epoxy resins.

The authors thank J. Asarou for his technical assistance.

References

1. Yu, L.; Dean, K.; Li, L. Prog Polym Sci 2006, 31, 576.
2. Meier, M. A. R.; Metzger, J. O.; Schubert, U. S. Chem Soc Rev 2007, 36, 1788.
3. American Soybean Association, ASA Soybean Success 2008 Report. http://www.soygrowers.com/publications/ASA2008Report.pdf (accessed July 2009).
4. Ministry of Agriculture, Livestock, Fisheries and Food (Secretaría de Agricultura, Ganadería, Pesca y Alimentos, SAGPyA), Annual Statistics of Production of Soybeans and Derivatives. http://www.sagpya.mecon.gov.ar (accessed July 2010).
5. Miyagawa, H.; Mohanty, A. K.; Burgueño, R.; Drzal, L. T.; Misra, M. Ind Eng Chem Res 2006, 45, 1014.
6. Park, S. J.; Jin, F. L.; Lee, J. R. Macromol Rapid Commun 2004, 25, 724.
7. Rüsch gen. Klaas, M.; Warwel, S. Ind Crop Prod 1999, 9, 125.
8. Montero de Espinosa, L.; Cronda, J. C.; Galia, M.; Cádiz, V. A. J Polym Sci Part A: Polym Chem 2008, 46, 6843.
9. Miyagawa, H.; Mohanty, A. K.; Misra, M.; Drzal, L. T. Macromol Mater Eng 2004, 289, 636.
10. Zhu, J.; Chandrashekhara, K.; Flanigan, V.; Kapila, S. J Appl Polym Sci 2004, 91, 3513.
11. Czub, P. Macromol Symp 2006, 242, 60.
12. Liu, Z. S.; Erhan, S. Z.; Calver, P. D. Compos A 2007, 8, 87.
13. Park, S. J.; Jin, F. L.; Lee, J. R. Mater Sci Eng A 2004, 374, 109.
14. Jin, F. L.; Park, S. J. Polym Int 2008, 57, 577.
15. Boquillon, N.; Fringant, C. Polymer 2000, 41, 8603.
16. Gerbase, A. E.; Petzhold, C. L.; Costa, A. P. O. J Am Oil Chem Soc 2002, 79, 797.
17. Miyagawa, H.; Misra, M.; Drzal, L. T.; Mohanty, A. K. Polym Eng Sci 2005, 45, 487.
18. Tran, P.; Graiver, D.; Narayan, R. J Appl Polym Sci 2006, 102, 69.
19. Sharma, B. K.; Liu, Z.; Adhvaryu, A.; Erhan, S. Z. J. Agric Food Chem 2008, 56, 3049.
20. dos Santos Martini, D.; Braga, B. A.; Samios, D. Polymer 2009, 50, 2919.

21. Reiznautt, Q. B.; Garcia, I. T. S.; Samios, D. Mater Sci Eng C 2009, 29, 2302.
22. Shogren, R. L.; Petrovic, Z.; Liu, Z.; Erhan, S. Z. J Polym Environ 2004, 12, 173.
23. Dogan, E.; Küsefoglu, S. J Appl Polym Sci 2008, 110, 1129.
24. Lukaszcryk, J.; Jaszcz, K. Macromol Chem Phys 2002, 203, 301.
25. In Annual Book of ASTM Standards; ASTM D 6110-04; American Society for Testing and Materials: West Conshohocken, PA, 2004.
26. In Annual Book of ASTM Standards; ASTM D 695-02; American Society for Testing and Materials: West Conshohocken, PA, 2002.
27. Trappe, V.; Buchard, W.; Steinmann, B. Macromolecules 1991, 24, 4738.
28. Rocks. J.; Rintoul, F.; Vohwinkel, F.; George, G. Polymer 2004, 4, 6799.
29. Musto, P.; Abbate, M.; Ragosta, G.; Scarinzi G. Polymer 2007, 48, 3703.
30. Thomas, R.; Yumei, D.; Yuelong, H.; Le, Y.; Moldenaers, P.; Weimin, Y.; Czigany, T.; Thomas, S. Polymer 2008, 49, 278.
31. Ratna, D. Polym Int 2001, 50, 179.
32. Mizutani, K. J Mater Sci 1993, 28, 2178.
33. Barton, A. F. M. Handbook of Solubility Parameters and Other Cohesive Parameters; CRC: Boca Raton, FL, 1985; p 142.
34. Hoppe, C. E.; Galante, M. J.; Oyanguren, P. A.; Williams, R. J. J.; Girard-Reydet, E.; Pascault, J. P. Polym Eng Sci 2004, 42, 2361.
35. Stefani, P. M.; Moschiar, S. M.; Aranguren, M. I. J Appl Polym Sci 2001, 82, 2544.
36. Jin, F.-L.; Park, S.-J. Mater Sci Eng A 2008, 478, 402.